Excited states of 8Be populated via the p(7Li, 4He)4He and p(7Li, 4He*)4He resonant reactions

Freer, Martin; Ashwood, Nicholas; Curtis, Neil; Munoz-Britton, Tomas; Wheldon, Carl; Ziman, Victor; Brown, S; Catford, WN; Patterson, NP; Thomas, JS; Weisser, DC

DOI:
10.1088/0954-3899/35/12/125108

Document Version
Publisher's PDF, also known as Version of record

Citation for published version (Harvard):
Freer, M, Ashwood, N, Curtis, N, Munoz-Britton, T, Wheldon, C, Ziman, V, Brown, S, Catford, WN, Patterson, NP, Thomas, JS & Weisser, DC 2008, 'Excited states of ^{8}Be populated via the $p(^{7}$Li, ^{4}He$)^{4}$He and $p(^{7}$Li, ^{4}He*$)^{4}$He resonant reactions', *Journal of Physics G: Nuclear and Particle Physics*, vol. 35, no. 12, 125108, pp. 1-10. https://doi.org/10.1088/0954-3899/35/12/125108

J. Phys. G: Nucl. Part. Phys. **35** (2008) 125108 (10pp) doi:10.1088/0954-3899/35/12/125108

Excited states of ^{8}Be populated via the $p(^{7}\mathrm{Li},^{4}\mathrm{He})^{4}\mathrm{He}$ and $p(^{7}\mathrm{Li},^{4}\mathrm{He}^{*})^{4}\mathrm{He}$ resonant reactions

M Freer[1], N I Ashwood[1], N Curtis[1], T Munoz-Britton[1], C Wheldon[1], V A Ziman[1], S Brown[2], W N Catford[2], N P Patterson[2], J S Thomas[2] and D C Weisser[3]

[1] School of Physics and Astronomy, University of Birmingham, Edgbaston, Birmingham, B15 2TT, UK
[2] School of Electronics and Physical Sciences, University of Surrey, Guildford, Surrey, GU2 7XH, UK
[3] Department of Nuclear Physics, Australian National University, Canberra, ACT 0200, Australia

Received 14 July 2008
Published 14 October 2008
Online at stacks.iop.org/JPhysG/35/125108

Abstract

A measurement of the $p(^{7}\mathrm{Li}, ^{4}\mathrm{He})^{4}\mathrm{He}$ resonant reaction on a thick mylar target was used to probe resonances in ^{8}Be in the excitation energy range 20–25 MeV. The ^{7}Li beams, of energies 25.8 and 58 MeV, were stopped in the target and the resulting α-particles were detected at zero degrees. Evidence was found for resonances at ∼20 and ∼25 MeV with $J^{\pi} = 0^{+}$ and 2^{+} character, respectively. A simultaneous measurement of the $p(^{7}\mathrm{Li}, ^{4}\mathrm{He}^{*} \rightarrow p + t)^{4}\mathrm{He}$ reaction was performed, in which one of the two final-state α-particles was produced in the 20.2 MeV excited state. These events were observed to arise from an excitation energy region 23–25 MeV and have been associated with the decay of the 25.2 MeV 2^{+} ^{8}Be resonance. The 25.2 MeV resonance is found to have a dominant $^{4}\mathrm{He} + ^{4}\mathrm{He}^{*}$ reduced width.

(Some figures in this article are in colour only in the electronic version)

1. Introduction

The structure of ^{8}Be has long been believed to be strongly linked with α–α clustering. The ground state sits above the α-decay threshold and has only a finite lifetime ($\Gamma = 5.57(0.25)$ eV) by virtue of the Coulomb barrier. This accords strongly with the Ikeda picture where cluster structure should be strongly manifested close to the cluster decay threshold [1]. The ground-state rotational band, with 2^{+} and 4^{+} members at 3.03 and 11.35 MeV, has a large moment of intertia commensurate with two 'touching' α-particles. This view of the nature of the ^{8}Be ground state is reinforced by the *ab initio* calculations using the Green's function Monte Carlo approach (GFMC) [2], where the α–α cluster structure is observed explicitly.

The ^{4}He nucleus has a rather robust character, which is in part why it is such a stable cluster. There is a 0^+ state at 20.2 MeV which corresponds to a 1p–1h excitation to the sd-shell, and has been associated with a breathing mode excitation [3], but has also been associated with a (3+1)-type cluster structure [4–6]. The latter description provides a good agreement with the electron inelastic scattering form factor. There is then a series of seven states ($T = 0, 0^-, 1^-, 2^-$; $T = 1, 0^-, 1^-, 2^-; 1^-$). These have been associated with a SU(4) spin–isospin supermultiplet [9], but are also well described by the 3+1 cluster model [5]. All of these states appear above the $p + t$ decay threshold, and given the isospin of the proton and triton, both $T = 0$ and $T = 1$ states would decay in this manner. An interesting test of the α–α cluster structure of the ^{8}Be ground state would be the search for states in ^{8}Be associated with the excitation of one of the clusters. This idea was explored theoretically (e.g. [10–12]) and experimentally (e.g. [13, 14]) some years ago, but no clear conclusions emerged. The existence of α-core excitations has been used to describe the excitations of the hypernucleus $^9_\Lambda$Be [7], which indicates the potential of this approach. In addition, quasi-free scattering measurements have an established tradition in terms of providing information of the degree of clustering in the ground state of, for example, ^{6}Li [8]. However, such techniques cannot be applied to the case of ^{8}Be.

Here we revisit this problem and present the analysis of the $p(^7\mathrm{Li}, ^4\mathrm{He})^4\mathrm{He}$ and $p(^7\mathrm{Li}, ^4\mathrm{He}^* \rightarrow p + t)^4\mathrm{He}$ reactions using the thick target resonant scattering approach. The reaction products are measured at zero degrees and a direct comparison between the two reaction channels has been made.

2. Experimental details

The measurements were performed using 25.8 and 58 MeV ^{7}Li beams from the ANU 14UD accelerator facility. The intensities were restricted to <1 enA to limit damage to the targets. The targets were constructed from 100 μm thick aluminized mylar sheets, $(C_9O_4H_8)_n$. The thickness of the aluminium was negligible and total thicknesses of 300, 600 and 800 μm were employed; the first for the lower beam energy, and the last two for the 58 MeV beam. These targets were designed to stop the beam and the beam current was monitored via an electrical contact to the target mechanism. The range of 25.8 and 58 MeV ^{7}Li nuclei in mylar was calculated to be 140 and 560 μm, respectively.

The detection system was placed on the beam axis directly behind the target. The telescope was composed of a four element detector telescope (illustrated in figure 1). The first element was a 70 μm thick double-sided silicon strip detector (DSSSD). This had a surface area of 5×5 cm^2 and was subdivided into 16 horizontal and 16 vertical strips on the front and rear of the detector, respectively. The second two elements of the telescope were strip detectors of a similar design but with a thickness of 1 mm. The final component was a 1 cm thick CsI detector to stop the most penetrating particles. The second strip detector was used in the calculation of the emission angles of the particles and was placed 12.85 cm from the target. The various elements were calibrated using α-sources and elastic scattering of ^{7}Li nuclei at 25.8 MeV. The energy resolution of the strip detectors was 200 keV.

3. Analysis and results

3.1. The $p(^7\mathrm{Li}, ^4\mathrm{He})^4\mathrm{He}$ *reaction*

The particle identification spectra for single events (events in which only one particle was registered in the telescope) are shown in figure 2 for the two beam energies. These spectra

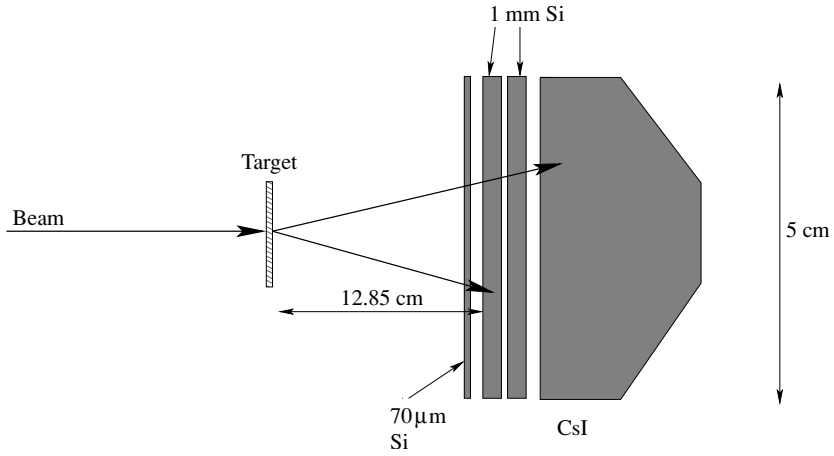

Figure 1. Detection setup. The beam was stopped by a thick mylar target. Beyond the target was a four element telescope. The first three elements were double-sided silicon strip detectors of thicknesses 70, 1000 and 1000 μm. The last component was a 1 cm thick (minimum thickness) CsI detector. Not to scale.

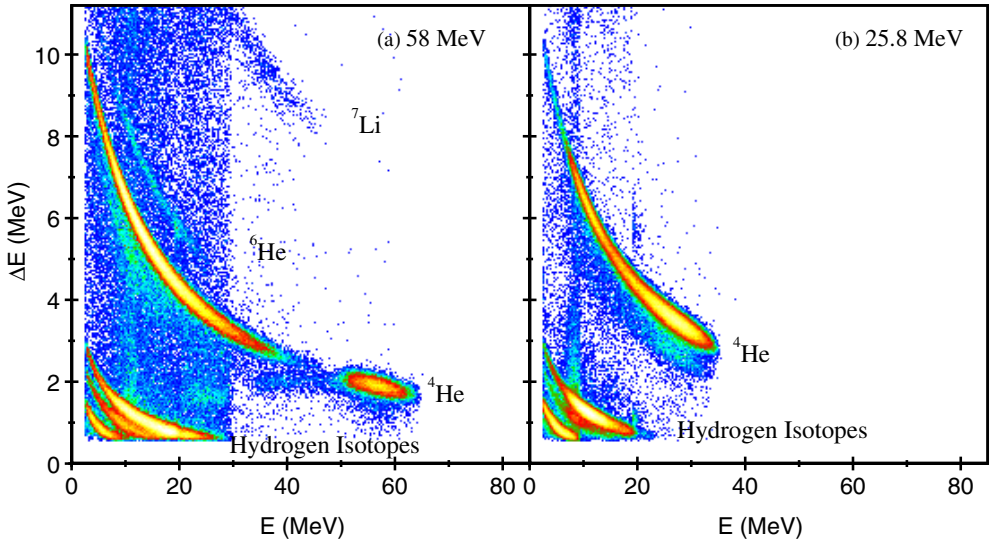

Figure 2. Particle identification spectra for the two different beam energies; (a) 58 MeV and (b) 25.8 MeV.

correspond to the energy of the first silicon detector (ΔE) plotted against the sum of the energies deposited in the remaining elements of the telescope. The loci corresponding to the three hydrogen isotopes can clearly be seen at $\Delta E < 3$ MeV. At higher values of energy loss the isotopes of helium 3, 4 and 6 are well resolved (the latter is only observed with the higher beam energy). There is also a locus which corresponds to ^{7}Li. This latter contribution arises from a small amount of slit scattering which results in ^{7}Li being scattered from the collimation system into the telescope, bypassing the target.

The strongest loci correspond to protons, tritons and α-particles. A large component of the α-particle and triton yields might be expected to arise from the break-up of the ^{7}Li projectile in the target. This reaction has a Q-value of -2.5 MeV. The $p(^7\mathrm{Li}, ^4\mathrm{He})^4\mathrm{He}$ reaction has a large, positive, Q-value of 17.35 MeV, which means that α-particles produced in this reaction are of much higher energy than those arising from the break-up. Indeed, this Q-value results in α-particles from this latter reaction having energies significantly higher than any of the possible contaminant reactions. An examination of both parts of figure 2 indicates an enhanced yield towards the high-energy end of the α-particle loci, this would be associated with resonance formation in ^{8}Be decaying to the 2α final state. It should be noted that some of the change of intensity towards the end of the locus in figure 2(a), $E > 45$ MeV, corresponds to a change in scaling factor for events in which the particles penetrated to the third element of the telescope (triggers associated with events which only passed through the first two elements of the telescope were pre-scaled down in intensity by a factor of $\sim$7).

Figures 3(a) and (b) show the energies and angles of the α-particles for the two beam energies. The energies of the α-particles have been corrected for their energy loss through the mylar foil, taking into account the interaction depth. In figure 3(a) the high-energy limit is observed to vary with angle and this corresponds closely to that calculated assuming the $p(^7\mathrm{Li}, ^4\mathrm{He})^4\mathrm{He}$ reaction. Reactions from other (heavier) target components give much flatter kinematic loci. Similarly, the high-energy dependence of the data for the lower energy beam are also well reproduced by the expected kinematics. Figure 3(c) shows the projections of (a) and (b) onto the energy axis with the lower energy data, below the punch-through energy, from (a) appropriately scaled. It should be noted that there is a *dead region* where the sensitivity of the telescope is reduced at the point where the energy of the α-particles is just sufficient to pass through the second detector to the third. The finite energy threshold on the third detector causes these events to be displaced to lower α-particle energies. This region is marked by two parallel dashed lines in figure 3(a). This effect is not observed for the 25.8 MeV data due to the lower energies of the particles in figure 3(b).

Figure 3(c) shows the two datasets combined, where they have been appropriately scaled for beam exposure and trigger pre-scale factors. The data appear to show resonance-like features with increased yield towards higher energies for the two datasets. These would correspond to resonant states in ^{8}Be. It should be noted that the highest energy α-particles are limited by the beam energy and that the peaks do not correspond to the full resonance line-shape, but rather the lower energy part of resonances in this region. Monte Carlo simulations of the ^{7}Li break-up reaction from carbon and oxygen components in the target indicate that at $E_{\mathrm{beam}} = 58$ MeV the break-up yield should reach up to $\sim$41 MeV. In the 58 MeV data (open diamonds in figure 3(c)) a steep rise in the cross section is observed close to this energy, which would account for the lack of observation of the lower energy resonance ($E(^4\mathrm{He}) \sim 37$ MeV) in the higher beam energy data. The break-up yield at $E_{\mathrm{beam}} = 25.8$ MeV is expected to appear close to the rise which is observed at $E(^4\mathrm{He}) = 22$ MeV.

Figure 4 shows the excitation energy spectrum of ^{8}Be for the data which has been superimposed with a calculation of the line-shapes of two of the known $T = 0$, even-spin and natural parity, resonances in ^{8}Be. Close to 20 MeV there are three possible resonances which could contribute to the data; 19.86 MeV (4^+, $\Gamma = 700(100)$ keV), 20.1 MeV (2^+, $\Gamma = 880(20)$ keV) and 20.2 MeV (0^+, $\Gamma = 720(20)$ keV) [15]. The 19.86 and 20.1 MeV resonances have been measured to have $\Gamma_\alpha/\Gamma_p = 2.3(0.5)$ and 4.5(0.6), respectively [16]. The properties of the three resonances are very similar (energies and widths) and are represented by a single Lorentzian profile in figure 4 (dashed line). At higher energies there exists a 2^+ resonance at 22.2 MeV, $\Gamma \sim 800$ keV, this does not seem to feature strongly in the present data, though this is located in the gap between the two measurements. Above 25 MeV there are 25.2 MeV,

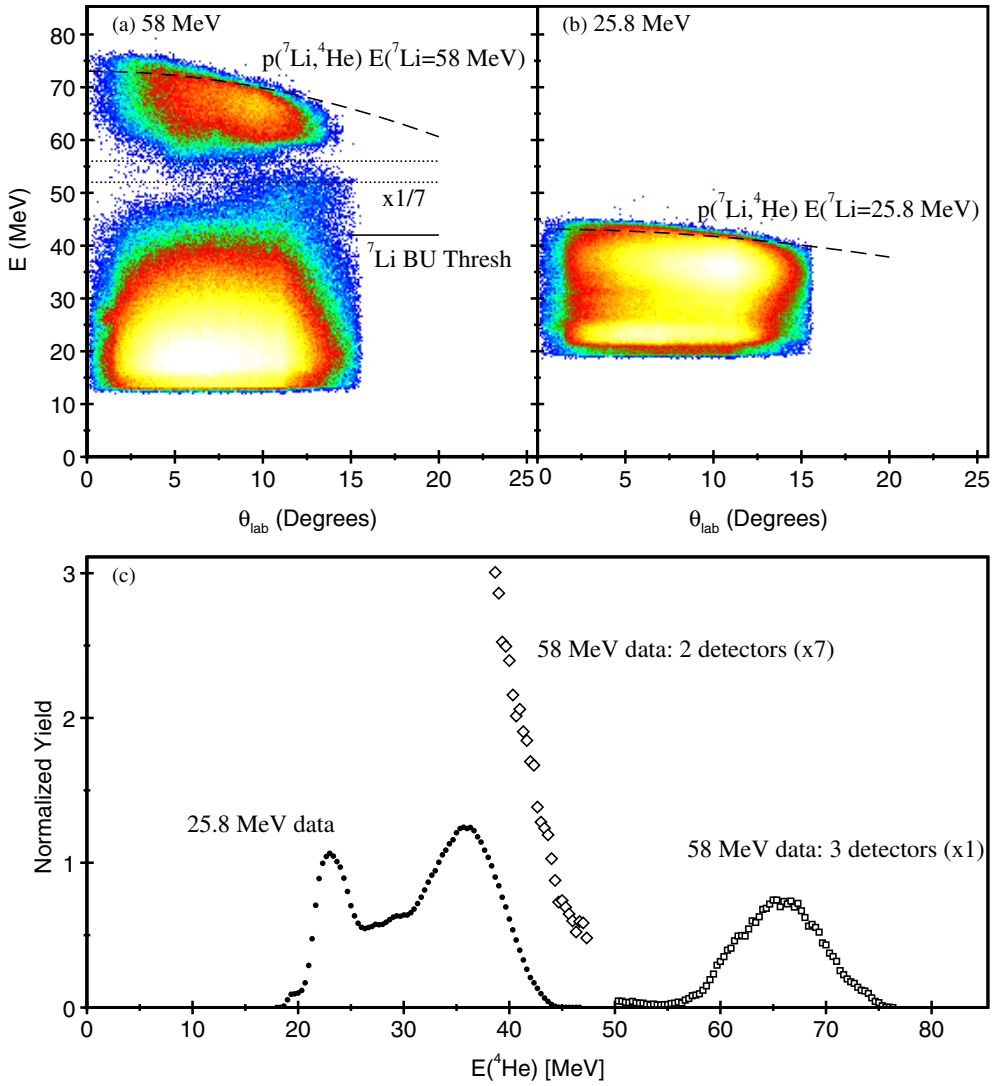

Figure 3. (a) Energies and angles of α particles for the 58 MeV data. The upper dashed line shows the kinematics predicted for the $p(^7\mathrm{Li}, ^4\mathrm{He})^4\mathrm{He}$ reaction. The *dead region* corresponding to the punch-through of the particles from the second to the third detector element is indicated by the dotted horizontal lines close to 53 and 56 MeV. The $^7\mathrm{Li} \rightarrow {}^4\mathrm{He} + {}^3\mathrm{H}$ threshold is indicated (^{7}Li BU Thresh) by a solid line. (b) Energies and angles of α particles for the 25.8 MeV data. The dashed line shows the kinematics predicted for the $p(^7\mathrm{Li}, ^4\mathrm{He})^4\mathrm{He}$ reaction. (c) The energies of the α-particles; filled circles are the 25.8 MeV events, open squares are the α-particles which penetrate to the third detector at 58 MeV and the open diamonds are the data at 58 MeV corresponding to events which stop in the second detector. The electronic scaling factor has been compensated for, i.e. the yield has been multiplied by a factor of 7.

2^+, and 25.5 MeV, 4^+ resonances, the latter of which are described as 'broad' [15]. These are represented in figure 4 with a Lorentzian with a width of 2 MeV—this width was found to provide a reasonable description of the present data.

The angular distributions have been examined in order to distinguish between the possible contributions to the present data (figure 5). Unfortunately the first minima in the angular

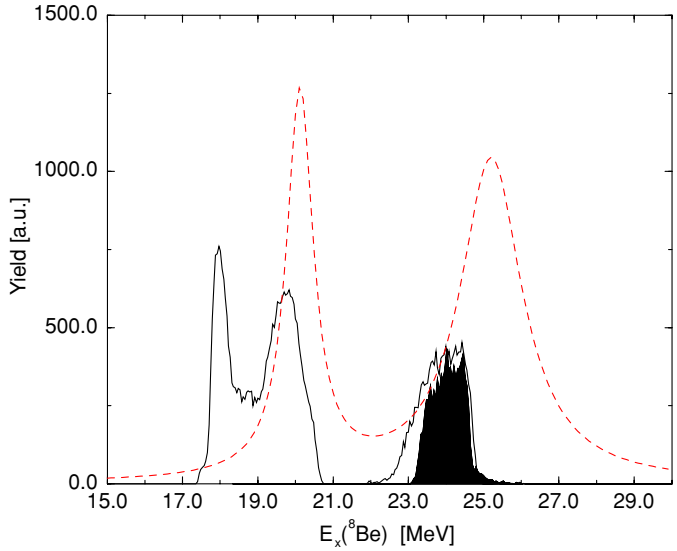

Figure 4. ^{8}Be excitation energy spectrum for the resonances observed in the $p(^{7}\mathrm{Li}, ^{4}\mathrm{He})^{4}\mathrm{He}$ reaction. The data corresponding to the $p(^{7}\mathrm{Li}, ^{4}\mathrm{He}^{*})^{4}\mathrm{He}$ reaction are shown by the filled histogram. The dashed line corresponds to the line-shape of resonances at 20.2 MeV and 25.2 MeV with widths of 0.72 MeV and 2 MeV, respectively—see text for details.

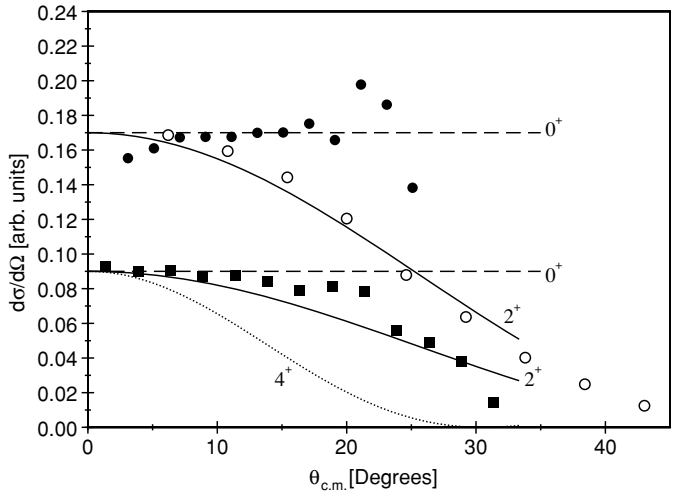

Figure 5. Angular distributions, corrected for detector acceptance, for the broad bumps in figure 3. The filled circles are the data for $E_x(^{8}\mathrm{Be}) \simeq 20$ MeV, the filled squares the $E_x(^{8}\mathrm{Be}) \simeq 24$ MeV data and the open circles are for the $^{4}\mathrm{He} + ^{4}\mathrm{He}^{*}$ channel. The dashed lines are the loci for a $J^{\pi} = 0^{+}$ resonance, the solid line $J^{\pi} = 2^{+}$ and the dotted line $J^{\pi} = 4^{+}$ (assuming a dominance of $m = 0$ decays). The statistical error bars are smaller than the data points.

distributions lie outside the present angular range. Nevertheless, the distributions for the *peak* at $E_x(^{8}\mathrm{Be}) \simeq 20$ MeV has a rather flat dependence which would suggest a lower spin resonance, certainly not 4^{+}, probably 0^{+} (assuming a dominance of $m = 0$ decays). The higher energy data indicate a trend closer to 2^{+} rather than 0^{+} or 4^{+}.

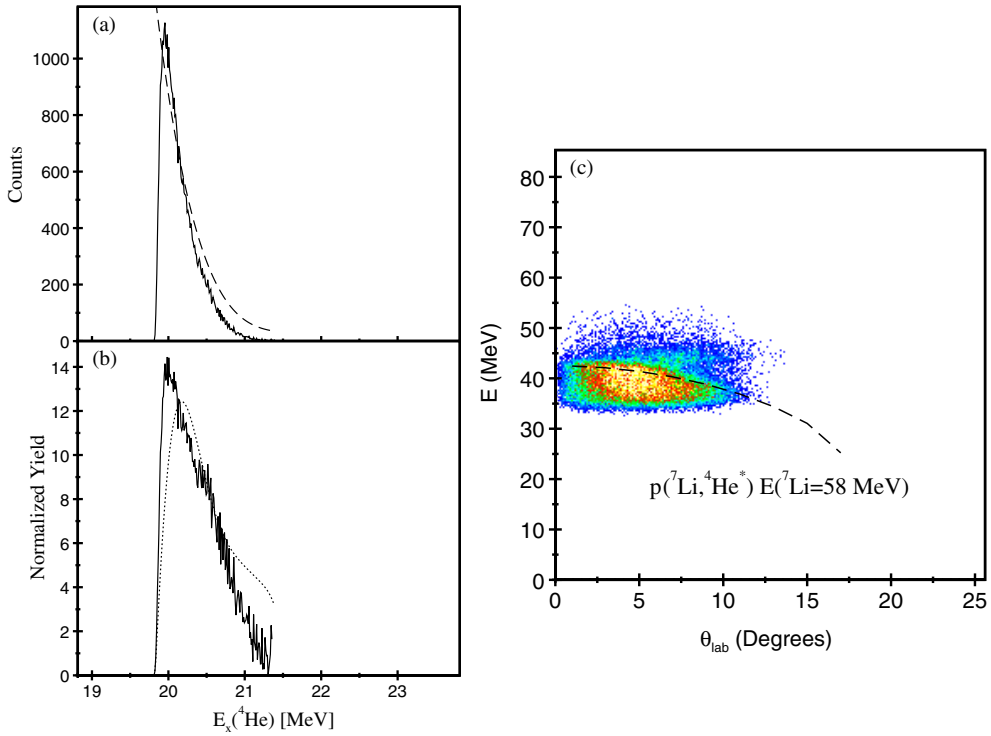

Figure 6. (a) ^{4}He excitation energy spectrum reconstructed from $p + t$ coincidences. The dashed line corresponds to the simulated detection efficiency. (b) The ^{4}He excitation energy spectrum normalized for the detection efficiency. The detection efficiency at 20 MeV is 30%. The dotted line is the predicted line-shape for the 20.21 MeV, 0^+ resonance in ^{4}He (see text for details). (c) The energy–angle dependence of the data with the kinematics associated with the $p(^7\text{Li}, ^4\text{He}^*)^4\text{He}$ reaction.

3.2. The $p(^7\text{Li}, ^4\text{He}^* \rightarrow p + t)^4\text{He}$ *reaction*

The pixellated nature of the telescope allows the identification of multiplicity 2 (and greater) events. In particular, in the $p(^7\text{Li}, ^4\text{He}^*)^4\text{He}$ reaction the excited α-particle will decay into $p + t$ since all of the excited states of ^{4}He lie above this decay threshold (at 19.815 MeV). The excitation energy spectrum reconstructed from the measurement of the energies and emission angles of protons and tritons is shown in figure 6(a), which was reconstructed using

$$E_x = 19.815 + (E_p + E_t) - E_\alpha, \tag{1}$$

where E_p and E_t are the energies of the proton and triton, respectively and the energy of the excited ^{4}He nucleus was reconstructed using the principle of conservation of momentum in the decay process;

$$E_\alpha = \frac{(\mathbf{p}_p + \mathbf{p}_t)^2}{2M_\alpha} \tag{2}$$

where $\mathbf{p}_p$ and $\mathbf{p}_t$ are the momenta of the proton and triton, respectively, and M_α is the mass of ^{4}He. The ^{4}He excitation energy spectrum can be seen to be concentrated close to the $p + t$ decay threshold (19.815 MeV). This is largely due to the nature of the detection efficiency which falls off quickly with increasing excitation energy. Monte Carlo simulations of the $p(^7\text{Li}, ^4\text{He}^* \rightarrow p + t)^4\text{He}$ reaction process, including the detector acceptances (both

energy and angular) are also shown in figure 6(a) (dashed line). It should be noted that it is only possible to observe this decay channel for the 58 MeV beam energy. The excitation energy spectrum normalized by the detection efficiency is shown in figure 6(b). The spectrum of states in ^{4}He which can decay into $p + t$ in this energy interval is dominated by the 20.21 MeV, 0^+, resonance ($\Gamma = 0.5$ MeV). The present experimental spectrum is compared to one deduced from the phase-shift analysis in [3] (dotted line in figure 6(b)). There is reasonably good agreement between the present spectrum and that from [3], which would indicate that the $p+t$ coincidences do arise from the decay of the ^{4}He 20.21 MeV first excited state. A second feature of the data which coincides with this interpretation is the energy–angle dependence of the events, which is shown in figure 6(c). As found in figure 3, the high-energy kinematic behaviour of the data is well reproduced assuming the ^{4}He + ^{4}He* final state and a ^{7}Li + p centre-of-mass energy corresponding to that of the initial beam energy. There is a small background component to the spectrum which can be observed above the kinematic locus of the $\alpha + \alpha^*$ reaction. The magnitude of this background contribution is estimated to be of the order of a few percent.

The location of these events in terms of the ^{8}Be excitation energy spectrum is shown in figure 4 (black histogram). This is seen to overlap completely with the coverage expected from the $p(^7\mathrm{Li}, ^4\mathrm{He})^4\mathrm{He}$ reaction. The angular distributions for these events are shown in figure 5 and indicate a resonance with $J^\pi = 2^+$. The relative decay strength for the decay from the 23–25 MeV region to the $\alpha+\alpha^*$ and $\alpha+\alpha$ channels has been estimated. This is based on selecting the yield over a common ^{8}Be excitation range (23–25 MeV) and normalizing the $\alpha + \alpha^*$ yield for the $p + t$ detection efficiency. The detection efficiency was weighted by the line-shape shown in figure 6(b) (dotted line). The $\alpha + \alpha$ yield was also corrected for the detector acceptance, taking into account the presence of identical final-state particles. This analysis gives a value of $\Gamma_{\alpha+\alpha^*}/\Gamma_{\alpha+\alpha} = 1.1(0.3)$. The energy lies substantially above the $\alpha+\alpha$ decay threshold and the penetrability through the $L = 2$ barrier at 24 MeV is calculated to be close to 50%. This would indicate that the $\alpha + \alpha^*$ reduced width is larger than that for $\alpha + \alpha$ and taking into account the phase-space factor $\gamma^2_{\alpha+\alpha^*}/\gamma^2_{\alpha+\alpha} = 4.8(1.3)$. This is in agreement with the observations from the $\alpha + \alpha$ resonant scattering measurements where it was found that the $\alpha + \alpha$ width of the 25.2 MeV, 2^+, resonance is smaller than the 2^+ resonances at lower energy [20].

4. Discussion

In the present measurements we find evidence for resonant-like structures in ^{8}Be observed in the $p(^7\mathrm{Li}, ^4\mathrm{He})^4\mathrm{He}$ reaction. These overlap with known resonances close to 20 and 25 MeV. The angular distributions correspond to a relatively narrow angular range but indicate that the lower energy peak is associated with $J^\pi = 0^+$ and the higher energy peak 2^+. Resonances in ^{8}Be have been observed in a number of reactions in this energy range. For example, resonant-like structures are observed in the $^6\mathrm{Li}(\mathrm{d}, ^4\mathrm{He})^4\mathrm{He}$ [17, 18], $^7\mathrm{Li}(p, ^4\mathrm{He})^4\mathrm{He}$ reaction [19] and ^{4}He+^{4}He resonant scattering [20]. The $^6\mathrm{Li}(\mathrm{d}, ^4\mathrm{He})^4\mathrm{He}$ and $^7\mathrm{Li}(p, ^4\mathrm{He})^4\mathrm{He}$ reactions indicate the presence of resonances with 0^+ and 2^+ character close to 20 MeV; 0^+, 2^+ and 4^+ close to 22 MeV and 2^+ at 25 MeV. There are complications in interpreting the data from these reactions (e.g. see [21]), and the most definitive are the ^{4}He + ^{4}He resonant scattering [20] measurements. These find three resonances close to 20 MeV with 0^+, 2^+ and 4^+ character, a 2^+ resonance close to 22 MeV and 2^+ and 4^+ resonances close to 25 MeV.

The present measurements are consistent with these studies and would appear to be associated strongly with the 0^+ resonance at 20.2 MeV and 2^+ at 25.2 MeV. The intermediate 2^+ resonance at 22.2 MeV largely coincides with a gap in the present acceptance.

Several measurements of the $\alpha + \alpha^*$ final state have also been performed (where the α-particle is produced in the first excited state, 20.2 MeV 0^+). For example, a broad structure is observed at 25 MeV in the ^{7}Li(p, ^{4}He*)^{4}He reaction by Warner *et al* [13], but at somewhat lower energy (24 MeV) in the same reaction by Čaplar *et al* [14]. In the latter case a definitive spin assignment was not found. It is observed in the ^{4}He + ^{4}He resonant scattering [20] that the $\alpha + \alpha$ width (both particles in their ground state) for the 2^+ resonance at this energy is much smaller than the other 2^+ states. This may correspond to an appreciable width for the $\alpha + \alpha^*$ channel. This is in agreement with the present measurements. It is likely that the resonance observed in the present measurements decaying to the $\alpha + \alpha^*$ and $\alpha + \alpha$ final state corresponds to the 25.2 MeV 2^+ resonance. It should also be noted that no other 0^+ resonances, aside from 20.2 MeV, have been observed in ^{8}Be, both in the present energy range and up to 35 MeV [20].

Given that cluster structures are expected to appear close to the associated cluster decay threshold (the Ikeda picture [1]) a cluster state based around the $\alpha + \alpha^*$ structure might be expected to appear close to the corresponding excited state of the α-particle; 20.2 MeV (neglecting the small 92 keV Q-value for the α-decay of ^{8}Be). Thus, the appearance of a 0^+ state in ^{8}Be at 20.2 MeV may not be coincidence. This state will have only a small width for decay to $\alpha + \alpha^*$ due to the proximity of the Coulomb barrier. A collective (rotational) excitation of this state would be at higher energy and thus may have a larger decay width to $\alpha + \alpha^*$. The 25.2 MeV state is observed strongly in the p(^{7}Li, ^{4}He*)^{4}He reaction, both in the present measurements and of [13], and is thus the best candidate for such a collective excitation. It should be noted that the measurements of Čaplar *et al* [14] do not show any significant decay strength for the 22.2 MeV, 2^+ state to the $\alpha + \alpha^*$ final state. The 0^+ and 2^+ states are separated by 5 MeV, which may be compared with 3.06 MeV for the ground-state rotational band. This would indicate a more compact configuration for a $\alpha + \alpha^*$ cluster structure than the ground state.

5. Summary and conclusions

The present measurements of the p(^{7}Li, ^{4}He)^{4}He and p(^{7}Li, ^{4}He*)^{4}He reactions, performed at $E_{\text{beam}} = 25.8$ and 58 MeV, are in good agreement with previous measurements and also $\alpha + \alpha$ resonant scattering studies. Evidence was found for resonant structures in ^{8}Be at 20 and 25 MeV are observed with $J^\pi = 0^+$ and 2^+, respectively. It is proposed that these resonances are associated with $\alpha + \alpha^*$ structure, the energy difference of which would suggest a more compact structure than appears in the ground state. Further measurements to extend the energy and angular range of the present measurements are planned. A natural extension of the present ideas would be the search for excitations of α-particles in the analogue of the 7.65 MeV Hoyle state in ^{12} C. Such states would exist at an energy close to 20.2 + 7.65 = 27.85 MeV, which lies very close to the $2\alpha + t + p$ decay threshold (27.087 MeV). Such a state, in principle, could be accessed through the $p + ^{11}$B reaction.

Acknowledgments

The authors wish to thank the staff of the Department of Nuclear Physics at the Australian National University for assisting with the running of the experiments. The financial support of the UK STFC (Science and Technology Facilities Council) is acknowledged. The experimental work was performed under a formal agreement between the STFC and ANU.

References

[1] Ikeda K, Tagikawa N and Horiuchi H 1968 *Prog. Theor. Phys. Suppl., Extra Numbers* 464
[2] Wiringa R B, Pieper S C, Carlson J and Pandharipande V R 2000 *Phys. Rev.* C **62** 014001
[3] Csótó A and Hale G M 1997 *Phys. Rev.* C **55** 2366
[4] Furutani H, Horiuchi H and Tamagaki R 1978 *Prog. Theor. Phys.* **60** 307
[5] Furutani H, Horiuchi H and Tamagaki R 1979 *Prog. Theor. Phys.* **62** 981
[6] Hiyama E, Gibson B F and Kamimura M 2004 *Phys. Rev.* C **70** 031001
[7] Yamada T, Ikeda K, Bando H and Motoba T 1988 *Phys. Rev.* C **38** 854
[8] Pugh H B, Watson J W, Goldberg D A, Roos P G, Bonbright D I and Riddle R A J 1969 *Phys. Rev. Lett.* **22** 408
[9] de Shalit A and Walecka J D 1966 *Phys. Rev.* **147** 763
[10] Fiebig H R and Timm W 1982 *Phys. Rev.* C **26** 2367
[11] Zahn W 1977 *J. Phys. G: Nucl. Phys.* **3** 9
[12] Hackenbroich H H, Seligman T H, Zahn W and Fick D 1976 *Phys. Lett.* B **62** 121
[13] Warner R E, Ball G C, Davies W G, Fergusonv A J and Forster J S 1979 *Phys. Rev.* C **19** 293
[14] Čaplar R, Gemmeke H, Lassen L, Weiss W and Fick D 1980 *Nucl. Phys.* A **342** 71
[15] Tilley D R, Kelley J H, Godwin J L, Millener D J, Purcell J E, Sheu C G and Weller H R 2004 *Nucl. Phys.* A **745** 155
[16] Pugach V M, Pavlenko Yu N, Prokopets A G, Vasilev Yu O, Kiva V A and Medvedev V I 1992 *Bull. Russ. Acad. Sci. Phys.* **56** 1768
[17] Freeman R M and Mani G S 1965 *Proc. Phys. Soc. Lond.* **85** 267
Tsan U C, Longequeue J P and Beaumevieille H 1969 *Nucl. Phys.* A **124** 449
[18] Darriulat P, Igo G, Pugh H and Holmgren H D 1965 *Phys. Rev.* **137** B315
[19] Kumar N and Barker F C 1971 *Nucl. Phys.* A **167** 434
[20] Bacher A D, Resmini F G, Conzett H E, de Swiniarski R, Meiner H and Ernst J 1972 *Phys. Rev. Lett.* **29** 1331
[21] Elwyn A J and Monahan J E 1979 *Phys. Rev.* C **19** 2114